Research Article

Amira A. Elabd* and Olivea A. Elhefnawy

Fluorescence quenching detection of UO_2^{2+} in aqueous solution based on an organic molecule probe of 6-chloro-2*H*-1,2,4-benzothiadiazine-7-sulfonamide 1,1-dioxide

https://doi.org/10.1515/revac-2021-0123
received October 17, 2020; accepted January 22, 2021

Abstract: A new organic molecule probe has been introduced as a "turn-off" fluorescent sensor to detect trace quantities of UO_2^{2+} in the presence of several transition metals with promising results. The procedure is based on quenching the fluorescence intensity of 6-chloro-2*H*-1,2,4-benzothiadiazine-7-sulfonamide 1,1-dioxide (**L**) in the presence of various UO_2^{2+} concentrations in methanol. The UO_2^{2+} and **L** species interact through electrostatic interaction between negatively charged nitrogen atom of the sulfonamide group of **L** and positively charged UO_2^{2+}, thus facilitating the non-radiative recombination of UO_2^{2+} and **L** through the charge transfer or electron transfer processes and leading to the fluorescence quenching of **L**. The mechanism of quenching was addressed and proved to be static quenching. The impressive quenching of the fluorescence intensity of **L** by different concentrations of UO_2^{2+} has been successfully used as a new sensor to measure UO_2^{2+} in methanol at λ_{ex} = 340 nm, λ_{em} = 380 nm with a linear dynamic range of 0.08–5.0 μM and detection limit and quantification limit of 0.0276 and 0.0837 μM, respectively. The **L** sensor shows interesting advantages compared to other developed sensors with adequate performance, such as broader linear range and lower detection limit, selectivity, and simplicity, which illustrate its useful practical use.

Keywords: fluorescence, UO_2^{2+}, quenching, assessment

*** Corresponding author: Amira A. Elabd,** Nuclear Safeguards and Physical Protection Department, Nuclear and Radiological Regulatory Authority (NRRA), P. O. Box 7551, Cairo, Egypt, e-mail: a.a.elabd@gmail.com, tel: +20-122-578-1529
Olivea A. Elhefnawy: Nuclear Safeguards and Physical Protection Department, Nuclear and Radiological Regulatory Authority (NRRA), P. O. Box 7551, Cairo, Egypt

1 Introduction

The fast development of nuclear industry, such as the extraction of uranium minerals, the generation of nuclear electricity, the treatment of spent fuel, and the manufacturing of nuclear weapons, has produced a residue of uranium pollution in the marine environment, posing a clear threat to the ecological system and to human and animal health [1]. In aqueous solution, uranium has many forms, and the most prevalent one is uranyl (UO_2^{2+}) [2–5]. The development of a fast and efficient analytical procedure for UO_2^{2+} recognition enables it to be measured at a very low concentration to avoid its adverse effects on the atmosphere and on the living organism at an early phase. Analytical techniques such as atomic absorption spectrometry [6,7], atomic emission spectrometry [8,9], or mass spectrometry [10,11] are routinely used in conjunction with a sample pretreatment scheme for high sensitivity UO_2^{2+} analysis. However, high cost, advanced and complicated devices, and the needs of skilled staff and well-equipped laboratories limit their use [12–14]. This causes problems for an on-site and real-time detection of heavy metal ions. Developing sensors with sensitivities comparable to those advanced instrumental techniques is a major challenge for a long time to come. This is because several metal ions have the same or almost ion radius, charging or other properties, making it hard to assess.

Fluorescence optical sensor is a very promising tool for potential practical applications due to its precision and its inherent sensitivity [15,16]. But fewer reports of UO_2^{2+} fluorescent sensors have been published. For instance, Chen et al. introduced an aggregation-induced emission-active sensor, 4-pethoxycarboxyl salicylaldehyde azine (PCSA), which displays high sensitivity towards UO_2^{2+} [17]. Also, 2,6-pyridinedicarboxylic acid (PDA) has been used as a fluorescence sensitizing agent for

UO_2^{2+} measurement by Maji and Viswanathan [18]. However, 2,6-pyridinedicarboxylic acid (PDA) interacts with various metal ions which hinder the detection of UO_2^{2+} in the presence of various competing ions. Wu et al. immobilized salophen and fluorescence-labelled oligonucleotide for separation and determination of trace UO_2^{2+} concentration [19]. Ganesh et al. used fluorescence enhancing reagent (sodium pyrophosphate) for the determination of UO_2^{2+} concentration during spent fuel reprocessing [20]. However, by using these sensors, the presence of some transition metals and thorium ions interfered with the UO_2^{2+} detection. In addition, additional chemicals (for instance, oligonucleotide, sodium pyrophosphate, and calcein) or tools are needed to achieve the required sensitivity and selectivity. Therefore, in the presence of transitional metals and less chemical uses, the development of highly selective and sensitive fluorescent sensors for UO_2^{2+} recognition remains a challenge.

In the literature, some thiol-based ligands have been found, which have been used for the detection of transition metal ions [21–23]. The present study used thiazide-based ligand as a new organic molecule probe [6-chloro-2*H*-1,2,4-benzothiadiazine-7-sulfonamide-1,1-dioxide (**L**)] for the assessment of UO_2^{2+}. The literature review and preliminary study indicated the following: first, **L** sensor belongs to the thiazide class and has strong fluorescence spectra due to high mobility of its π-electron and high quantum yield. Second, **L** sensor has high molar absorptivity, which is preferred because the absorption light is increasing at a given wavelength. Third, the preliminary studies of the absorbance and fluorescence emission spectra of **L** have shown variations that exist when UO_2^{2+} is gradually added to **L** and the fluorescence emission intensity of **L** is decreased. Therefore, the concentration of UO_2^{2+} could thus be detected quantitatively. In this regard, **L** was studied for the application of a new organic molecule probe for spectrofluorometric assessment of UO_2^{2+} in aqueous solution.

2 Experimental

2.1 Materials

The chemicals used in the tests were of analytical grade with no further purification. 6-Chloro-2*H*-1,2,4-benzothiadiazine-7-sulfonamide 1,1-dioxide (**L**) was purchased from Sigma-Aldrich. Uranyl nitrate hexahydrate, $UO_2(NO_3)_2{\cdot}6H_2O$, was manufactured by Mallinckrodt Company. All the other chemicals used in this study were purchased from Alpha Company.

2.2 Instruments

Fluorescence emission spectra were measured using Meslo-PN (Lumina fluorescence Spectrometer; Thermo Scientific, USA). Both emission and excitation slits were at 5.0 nm. The absorption spectra were measured using UV-Vis Evolution 300 (Thermo Fisher Scientific Company, UK). As a reference, UO_2^{2+} was determined by inductively coupled plasma optical emission spectrometry (ICP-OES) (iCAP 6500 ICP-OES; Thermo Fisher Scientific, UK). Experiments were carried out in safeguards destructive analysis lab (ETZ-, KMP-I), Nuclear and Radiological Regulatory Authority.

2.3 Analytical procedures

In order to assess the UO_2^{2+} concentration by **L** sensor, a stock solution of UO_2^{2+} (100 μM) was prepared by dissolving an accurately weighed amount of uranyl nitrate hexhydrate ($UO_2(NO_3)_2{\cdot}6H_2O$) in deionized water containing few drops of concentrated sulphuric acid and standardized by a known method [24]. All working solutions were prepared by diluting the stock solution suitably with deionized water to give various concentrations of UO_2^{2+} from 0.08 to 5.0 μM. These various concentrations of UO_2^{2+} were added to **L** (1.0 mL, 100 μM). The solutions have been mixed with 10 mL of methanol. Measurements of the fluorescence emission intensities were carried out at λ_{ex} = 340 nm, λ_{em} = 380 nm, and 1 min (to reach the equilibrium). The linear range of the fluorescence emission intensity of **L** sensor was observed between 0.08 and 5.0 μM of UO_2^{2+} concentrations.

3 Results and discussion

3.1 Preliminary studies

6-Chloro-2*H*-1,2,4-benzothiadiazine-7-sulfonamide 1,1-dioxide (**L**) belongs to the thiazide class. Clearly, it emitted fluorescence as it possessed conjugated functional groups. In addition, its molar absorption is a factor deciding the

selection of **L** to be studied as a fluorescence sensor. High molar absorption of **L** is favoured because at a specified wavelength it enhances the absorption of light, so as it interacts with the target analyte, the sensitivity of **L** enhances. The molar absorptivity of **L** is 2.0×10^4 L/mol cm according to Jothieswari et al. [25].

The variations in the absorption and fluorescence emission spectra that appear after the addition of UO_2^{2+} to **L** (10 μM) have been examined in order to determine that **L** can be used as a sensitive fluorescent sensor for UO_2^{2+}.

The absorbance spectra of **L** and UO_2/**L** are shown in Figure 1. The **L** shows three absorption bands, at 230, 270, and 318 nm. This finding was similar to the findings of the literature. When adding UO_2^{2+} to **L**, the absorption band intensity increased at 230 nm and the absorption band intensity decreased at 318 nm, which is a possible indicator of the formation of UO_2/**L** species.

Fluorescence emission spectra of **L** in the presence of various concentrations of UO_2^{2+} (8.0×10^{-8}, 3.0×10^{-7}, 6.0×10^{-7}, 9.5×10^{-7}, 1.5×10^{-6}, 2.3×10^{-6}, 2.8×10^{-6}, 3.5×10^{-6}, and 5.0×10^{-6} M, respectively) are shown in Figure 2. At an excitation wavelength 340 nm, the **L** sensor shows a characteristic fluorescent emission band at 380 nm.

The experimental results show that with the increase in the UO_2^{2+} concentration, the fluorescence emission intensity decreases and is fully quenched at a UO_2^{2+} concentration of 60.0 μM. This indicates that the fluorescence quenching ability of **L** sensor is good in the presence of UO_2^{2+}. In addition, in the UO_2^{2+} concentration range of 0.08–5.0 μM, the intensity of the fluorescence emission is

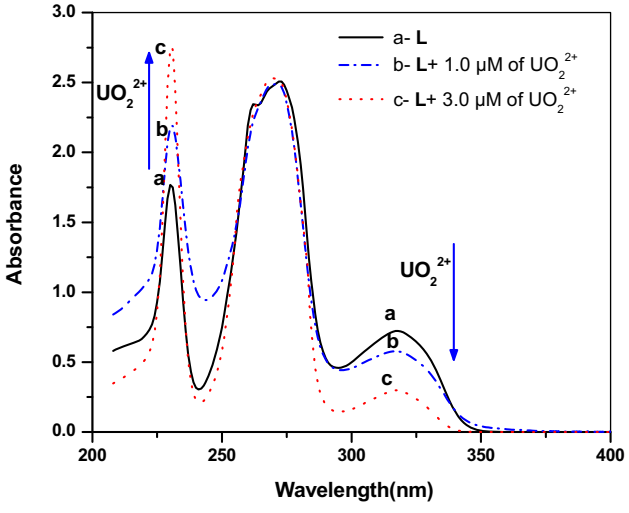

Figure 1: Absorbance spectra of the **L** sensor in the presence of different concentrations of UO_2^{2+}.

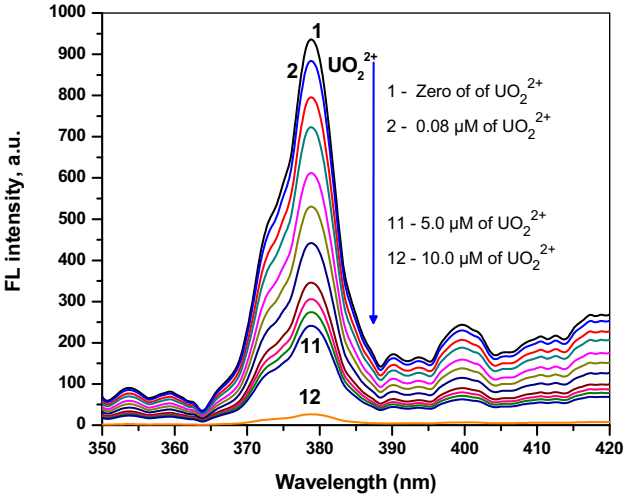

Figure 2: Fluorescence emission spectra of the **L** sensor in the presence of different concentrations of UO_2^{2+} at $\lambda_{ex}/\lambda_{em}$ = 340/380 nm.

linearly quenched. The UO_2^{2+} and **L** species interact through electrostatic interaction between positively charged UO_2^{2+} and negatively charged nitrogen atom of the sulfonamide group of **L**. It reveals that it is possible to use the chelating reaction between UO_2^{2+} and **L** to develop a fluorescence sensor for UO_2^{2+} determination. Since the absorbance intensity of **L** at λ = 318 nm decreased, and fluorescence emission intensity of **L** at $\lambda_{ex}/\lambda_{em}$ = 340/380 nm decreased as a function of UO_2^{2+} concentration, both indicated the prevalent formation of a UO_2/**L** species.

3.2 Mechanism

Scheme 1 shows the mechanism of UO_2^{2+} assessment using **L** as a fluorescent probe. Initially, when **L** was free in aqueous solution, they showed strong fluorescence intensity at $\lambda_{ex}/\lambda_{em}$ = 340/380 nm. In the presence of UO_2^{2+}, the fluorescence of **L** was quenched significantly. The results indicate that UO_2^{2+} induced fluorescence quenching of **L** by the chelation of positively charged UO_2^{2+} with negatively charged nitrogen atom of the sulfonamide group of **L**, thus facilitating the non-radiative recombination of UO_2^{2+} and **L** through the charge transfer or electron transfer processes and leading to the fluorescence quenching of **L**. Job's method of continuous variation was used to study stoichiometry. The plot of absorbance against the UO_2^{2+} mole fraction has shown that the complex formation between UO_2^{2+} and **L** is with a molar ratio of 1:2. Also, the reaction between UO_2^{2+} and **L** was studied by spectrofluorometry at

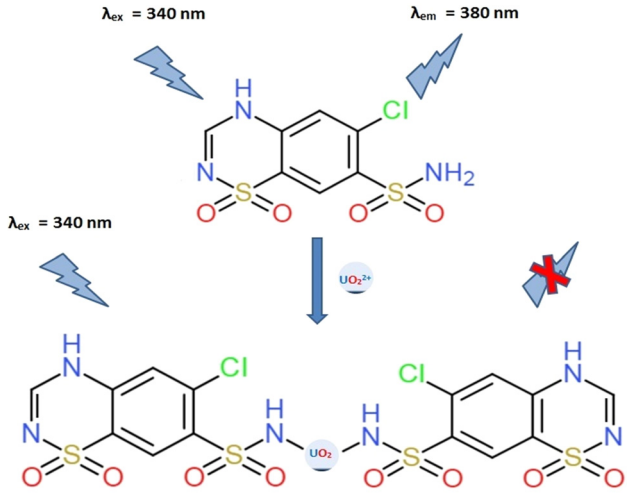

Scheme 1: A schematic representation of the proposed quenching mechanism of the **L** sensor with UO_2^{2+}.

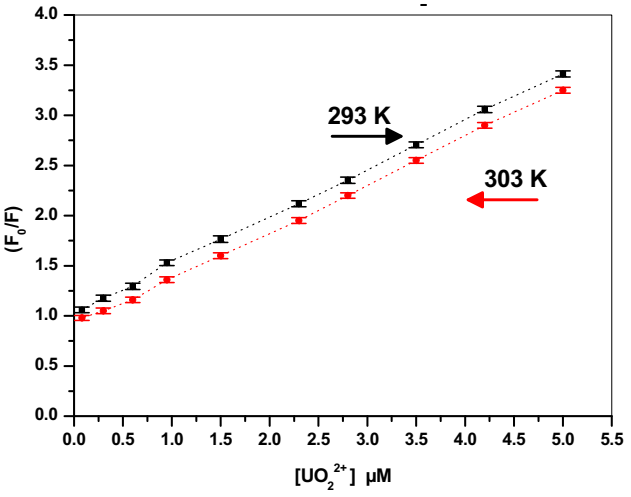

Figure 3: Stern–Völmer's plot of F_0/F versus [Q] at two different temperatures (293 and 303 K) (values are mean of five replicates), and all the RSD values are less than 2.0%.

different temperatures (293 and 303 K) (Figure 3) with the Stern–Völmer equation to understand the fluorescence quenching mechanism [26,27]:

$$\left[\left(\frac{F_0}{F}\right)\right] = 1 + K_{sv}[Q], \quad (1)$$

where F_0 and F are the fluorescence emission intensities of **L** in the absence and presence of UO_2^{2+}, respectively, Q is the quencher concentration of UO_2^{2+}, and K_{sv} is the constant of Stern–Völmer. Stern–Völmer's plot of F_0/F versus [Q] at different temperatures (293 and 303 K) is shown in Figure 3. And the calculated K_{sv} are 4.8×10^5 and 4.6×10^5 mol^{-1} at 293 and 303 K, respectively. This result indicates that there is a good agreement between quenching process and the Stern–Völmer equation, which is an indicator for static quenching mechanism because K_{sv} decreases with increase in temperature.

3.3 Inner filter effect (INF)

In fluorescence spectroscopy, the INF is a significant issue that especially affects spectral measurements. UO_2^{2+} is a fluorescent species and has absorption and fluorescence spectra. The steps that are being carried out in the experimental work to avoid INF are as follows: (1) choose sample with very low concentration to avoid primary INF and (2) select a particular excitation wavelength to reduce the absorption of the sample. The excitation is decreased to 80 nm (λ_{ex} = 340) below the absorption maximum of UO_2^{2+} (420 nm) to avoid secondary INFs.

3.4 Parameter study

3.4.1 Solvent effect

The **L** sensor showed the fluorescence emission spectra at λ_{ex} = 340 nm in different solvents. The influences of the solvent on the fluorescence emission intensity of **L** sensor are shown in Figure 4. The results showed that the fluorescence emission intensity of the **L** sensor is much higher in methanol than in other solvents. These could

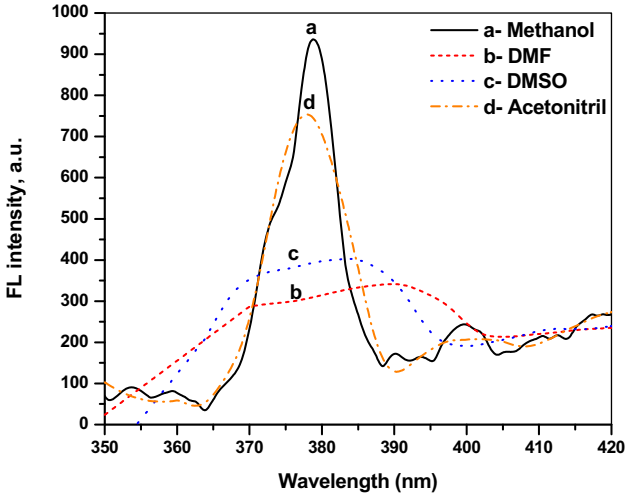

Figure 4: Fluorescence emission spectra of the **L** sensor in the presence of different solvents at $\lambda_{ex}/\lambda_{em}$ = 340/380 nm.

be due to various influence factors of solvent such as dielectric constant, polarity, etc. The dielectric constant and polarity of methanol (ε = 33, polarity = 0.762), acetonitrile (ε = 37.5, polarity = 0.46), DMF (ε = 36.71, polarity = 0.386), and DMSO (ε = 47.24, polarity = 0.444), respectively, indicate that the fluorescence quantum yield of **L** is increasing with the decrease in the solvent dielectric constant and with the increase in solvent polarity. In addition, **L** is more soluble in methanol. Thus, the high fluorescence quantum yields in methanol could be anticipated, and methanol was selected as the best solvent.

3.4.2 Concentration effect

In order to determine the influence of the concentration of **L** sensor, three concentrations of **L** at 20.0, 10.0, and 6.0 μM were studied. The linear range is 0.05–10.0 μM (RSD 1.04%) at the concentration of 20.0 μM, 0.08–5.0 μM (RSD 1.13%) at the concentration of 10.0 μM, and 0.06–3.0 μM (RSD 1.64%) at the concentration of 6.0 μM. By taking into consideration, in terms of linear range, detection limit, and response time, a good linear relationship is found between fluorescence emission intensity and **L** concentration. For further examination, the concentration of 10.0 μM for the **L** sensor was selected.

3.4.3 Selectivity study

An important property of the sensor is its selectivity to the analyte compared with other competing metal ions. Interference experiments for the determination of UO_2^{2+} in spiked methanol are conducted prior to the development of the **L** sensor.

The effects of various potential metal ions (aluminium, barium, calcium, cadmium, cobalt, cupper, chromium, iron, lanthanum, magnesium, manganese, nickel, and zinc) likely present in actual samples are investigated by injecting them into solutions containing 5.0 μM of UO_2^{2+} and by handling them as mentioned in the earlier procedure. The tolerance limit is the maximum amount of an ion that causes an error not greater than 5% in the fluorescence emission intensity of the consequent solutions. The findings indicate that the concentrations of aluminium (3.0 mg/L), barium (24.0 mg/L), calcium (22.0 mg/L), cadmium (15.0 mg/L), cobalt (11.0 mg/L), cupper (12.0 mg/L), chromium (4.0 mg/L), iron (3.0 mg/L), lanthanum (1.0 mg/L), magnesium (17.0 mg/L), manganese (17.0 mg/L), nickel (13.0 mg/L), and zinc (12.0 mg/L) have little effect on the **L** sensor fluorescence emission intensity, indicating that the **L** sensor has sufficient selectivity for UO_2^{2+} assessment.

3.5 Analytical figures of merit

The analytical parameters are measured in order to apply the fluorescent **L** sensor for UO_2^{2+} assessment. As shown in Figure 3, a good linear relation was obtained between F_0/F versus UO_2^{2+} concentration at 293 K. The regression equation was $F_0/F = 1.0326 + 4.8 \times 10^5 [UO_2^{2+}]$ (R^2 = 0.9992) within a concentration range of 0.08–5.0 μM. The limit of detection (LOD) is defined as the lowest amount of analyte in a sample, which can be detected but not necessarily quantitated as an exact value. The limit of quantification (LOQ) is defined as the lowest amount of analyte in a sample, which can be quantitatively determined with suitable precision and accuracy. In order to show the sensor constraint, LOD and LOQ were also calculated. According to the ICH guidance, LOD = $3.3S/b$ and LOQ = $10S/b$ (where S is the standard deviation and b is the slope) are tabulated in Table 1. These results suggested that the **L** sensor could be used as a tool for the assessment of UO_2^{2+} at very low concentration levels.

3.6 Application

In order to investigate the validity of the **L** sensor to various real aqueous samples, the various R&D samples are assessed by the **L** sensor and compared with the ICP-OES analysis. The various R&D samples spiked with UO_2^{2+} at different concentrations (0.10, 0.30, and 0.50 μM). The

Table 1: Analytical characteristics of **L** with UO_2^{2+}

Parameter	Value
λ_{ex} (nm)	340
λ_{em} (nm)	380
Linear range (M)	8.0×10^{-8}–5.0×10^{-6}
Limit of detection (LOD) (M)	2.76×10^{-8}
Limit of quantification (LOQ) (M)	8.37×10^{-8}
Standard deviation (SD)	0.004
Variance (SD^2)	1.6×10^{-5}
Correlation coefficient (R^2)	0.9992

Table 2: Application of **L** chemosensor for assessment of UO_2^{2+} in different samples

Sample	UO_2^{2+} spiked[a]	Proposed measured (n = 5)			Reference measured (n = 5)		
		UO_2^{2+} average measured[a] ± SD[b]	Recovery%	RSD%[c]	UO_2^{2+} average measured[a] ± SD[b]	Recovery%	RSD%[c]
S1	10	10.5 ± 0.23	105.0	2.19	10.2 ± 0.09	102.0	0.88
	30	31.1 ± 0.34	103.7	1.09	30.5 ± 0.23	101.7	0.75
	50	52.4 ± 0.67	104.8	1.27	50.6 ± 0.41	101.2	0.81
S2	10	10.4 ± 0.19	104.0	1.83	10.2 ± 0.08	102.0	0.78
	30	31.0 ± 0.34	103.3	1.09	30.3 ± 0.22	101.0	0.73
	50	51.8 ± 0.49	103.6	0.95	50.8 ± 0.39	101.6	0.76
S3	10	10.4 ± 0.18	104.0	1.73	10.2 ± 0.08	102.0	0.78
	30	31.2 ± 0.34	104.0	1.09	30.4 ± 0.20	101.3	0.66
	50	52.3 ± 0.50	104.6	0.96	50.7 ± 0.38	101.4	0.75
Tap water	10	9.57 ± 0.12	95.7	1.24	9.87 ± 0.09	98.7	0.93
	30	28.7 ± 0.31	95.6	1.09	28.9 ± 0.23	96.5	0.81
	50	47.9 ± 0.87	95.8	1.83	48.8 ± 0.38	97.6	0.78
Seawater	10	10.3 ± 0.13	103.4	1.26	10.2 ± 0.11	102.3	1.08
	30	31.4 ± 0.36	104.7	1.16	30.9 ± 0.31	103.1	1.01
	50	52.4 ± 0.66	104.8	1.26	51.4 ± 0.48	102.8	0.93

[a] The values are multiplied by 10^{-8} M. [b] SD, standard deviation, the values are multiplied by 10^{-8} M. [c] %RSD, relative standard deviation.

L sensor was added to the sample and mixed with 10 mL of methanol and then left for 1 min before measurement of the intensity of fluorescence. Table 2 shows the resulting data obtained. It was indicated that the recovery values are in the range of 95.6–105%. Also, the various R&D samples and their spiked samples are measured by ICP-OES analysis.

The results reveal that the UO_2^{2+} concentration detected from the **L** sensor was in a good agreement with the concentration results using the ICP-OES analysis. To check the accuracy of **L** sensor, the recovery results and the results from ICP-OES are used. The precision of the **L** sensor was measured and the three measurements were recorded as relative standard deviation (RSD%) values. The results of RSD% were lesser than 2.5%. These findings indicate that the procedure is precise and can be used for UO_2^{2+} assessment.

Further study is carried out by comparing the analytical parameters of the **L** sensor with some of other sensors developed, as shown in Table 3 [17,18,28–33]. The table reveals that, with adequate performance, the **L** sensor has impressive features, including a broader linear range and a lower detection limit, good selectivity, and remarkable simplicity.

Table 3: Comparison of the analytical parameters of **L** chemosensor with some of the developed optical sensors

Active material	Linear range (M)	Interfering ions	References
PCSA	3.7×10^{-9}–9.2×10^{-8}	Cu^{2+}	[17]
2,6-Pyridinedicarboxylic acid	2.6×10^{-7}–8.8×10^{-6}	Tb^{3+}	[18]
Tetraphenylethene (TPE) modified with 2-(4,5-dihydrothiazol-2-yl) phenol	1.0×10^{-6}–2.0×10^{-5}	—	[28]
Porphyrin-terminated polymeric	10^{-7}–10^{-3}	Cu^{2+}, Fe^{3+}, Ni^{2+}, Zn^{2+}	[29]
Cyclic peptide	3.6×10^{-7}–4.2×10^{-5}	—	[30]
Trimetazidine	4.9×10^{-8}–1.7×10^{-6}	Th^{4+}, Al^{3+}, Fe^{3+}	[31]
Clopidogrel	1.0×10^{-9}–4.0×10^{-6}	Th^{4+}, some transition metals	[32]
Furosemide	7.0×10^{-7}–4.0×10^{-6}	Al^{3+}, Fe^{3+}, some transition metals	[33]
6-Chloro-2*H*-1,2,4-benzothiadiazine-7-sulfonamide-1,1-dioxide	8.0×10^{-8}–5.0×10^{-6}	Al^{3+}, Fe^{3+}, some transition metals	This work

4 Conclusion

A new turn-off **L** sensor is studied with regard to the potential application as a fluorescence quenching sensor for UO_2^{2+}. In particular, **L** sensor presents sensitivity and selectivity to UO_2^{2+} (the detection limit is 0.0276 μM), which is among the best reported results. From this, it was believed that the fluorescence **L** would be providing a promising and practical UO_2^{2+} sensing material.

Funding information: The authors state no funding involved.

Author contributions: Amira A. Elabd: conceptualization, methodology, investigation, writing – original draft, formal analysis, and writing – review and editing; Olivea A. Elhefnawy: conceptualization, methodology, investigation, writing – original draft, formal analysis, and writing – review and editing.

Conflict of interest: The authors state no conflict of interest.

Data availability statement: All data generated or analysed during this study are included in this published article.

References

[1] Xie Y, Chen C, Ren X, Wang X, Wang H, Wang X. Emerging natural and tailored materials for uranium-contaminated water treatment and environmental remediation. Prog Mater Sci. 2019;103:180–234.
[2] Burns PC, Ewing RC. Nuclear fuel in a reactor accident. Science. 2012;335:1184–8.
[3] Nassab HR, Souri A, Javadian A, Amini MK. A novel mercury-free stripping voltammetric sensor for uranium based on electropolymerized N-phenylanthranilic acid film electrode. Sensor Actuat B Chem. 2015;215:360–7.
[4] Geipel G. Some aspects of actinide speciation by laser-induced spectroscopy coord. Chem Rev. 2006;250:844–54.
[5] Rathore DPS. Advances in technologies for the measurement of uranium in diverse matrices. Talanta. 2008;77:9–20.
[6] Yildiz E, Sacmaci S, Kartal S, Sacmaci M. A new chelating reagent and application for coprecipitation in food samples by FAAS. Food Chem. 2016;194:143–8.
[7] Yang S, Jiang S, Hu K, Wen X. Investigation of dispersive solid-phase extraction combined with slurry sampling thermo spray flame furnace atomic absorption spectrometry for the determination of cadmium. Microchem J. 2020;154:104542.
[8] Balaram V. Recent advances in the determination of elemental impurities in pharmaceuticals-status, challenges and moving frontiers. Trend Anal Chem. 2016;80:83–95.
[9] Barin JS, Mello PA, Mesko MF, Duarte FA, Flores EMM. Determination of elemental impurities in pharmaceutical products and related matrices by ICP-based methods: a review. Anal Bioanal Chem. 2016;408:4547–66.
[10] Chandrasekaran K, Karunasagar D, Arunachalam J. Dispersive liquid–liquid micro extraction of uranium(VI) from groundwater and seawater samples and determination by inductively coupled plasma–optical emission spectrometry and flow injection–inductively coupled plasma mass spectrometry. Anal Methods UK. 2011;3:2140–7.
[11] Moeser C, Kautenburger R, Philipp Beck H. Complexation of europium and uranium by humic acids analyzed by capillary electrophoresis-inductively coupled plasma mass spectrometry. Electrophoresis. 2012;33:1482–7.
[12] Saha A, Deb SB, Sarkar A, Saxena MK, Tomar BS. Simultaneous preconcentration of uranium and thorium in aqueous samples using cloud point extraction. RSC Adv. 2016;6:20109–19.
[13] Zhang H, Cheng X, Chen L, Mo F, Xu L, Fu F. Magnetic beads-based DNA hybridization chain reaction amplification and DNAzyme recognition for colorimetric detection of uranyl ion in seafood. Anal Chim Acta. 2017;956:63–9.
[14] Saha A, Debnath T, Neogy S, Ghosh HN, Saxena MK, Tomar BS. Micellar extraction assisted fluorometric determination of ultra trace amount of uranium in aqueous samples by novel diglycolamide-capped quantum dot nanosensor. Sensor Actuat B Chem. 2017;253:592–602.
[15] Gui R, Jin H, Bu X, Fu Y, Wang Z, Liu Q. Recent advances in dual-emission ratiometric fluorescence probes for chemo/biosensing and bioimaging of biomarkers. Coordin Chem Rev. 2019;383:82–103.
[16] Gui R, Jin H. Recent advances in synthetic methods and applications of photo-luminescent molecularly imprinted polymers. J Photochem Photobiol C. 2019;41:100315.
[17] Chen X, He L, Wang Y, Liu B, Tang Y. Trace analysis of uranyl ion (UO_2^{2+}) in aqueous solution by fluorescence turn-on detection via aggregation induced emission enhancement effect. Anal Chim Acta. 2014;847:55.
[18] Maji S, Viswanathan KS. Sensitization of uranium fluorescence using 2,6-pyridinedicarboxylic acid: application for the determination of uranium in the presence of lanthanides. J Lumin. 2009;129:1242.
[19] Wu M, Liao L, Zhao M, Lin Y, Xiao X, Nie C. Separation and determination of trace uranium using a double-receptor sandwich supramolecule method based on immobilized salophen and fluorescence labeled oligonucleotide. Anal Chim Acta. 2012;729:80–4.
[20] Ganesh S, Khan F, Ahmed MK, Velavendan P, Pandey NK, Mudali UK, et al. Determination of ultra traces amount of uranium in raffinates of Purex process by laser fluorimetry. J Radioanal Nucl Chem. 2012;292:331–4.
[21] Nalawade RA, Nalawade AM, Kamble GS, Anuse MARapid. Synergistic extractive spectrophotometric determination of copper(II) by using sensitive chromogenic reagent N″,N″-bis [(E)-(4-fluorophenyl) methylidene] thiocarbonohydrazide. Spectrochim Acta A. 2015;146:297–306.
[22] Kamble GS, Kolekar SS, Anuse MA. Synergistic extraction and spectrophotometric determination of copper(II) using

1-(2,4-dinitro aminophenyl)-4,4,6-trimethyl-1,4-dihydropyrimidine-2-thiol: Analysis of alloys, pharmaceuticals and biological samples. Spectrochim Acta A. 2011;78:1455–66.
[23] Kamble GS, Kolekar SS, Han SH, Anuse MA. Synergistic liquid–liquid extractive spectrophotometric determination of gold (III) using 1-(2,4-dinitro aminophenyl)-4,4,6-trimethyl-1,4-dihydropyrimidine-2-thiol. Talanta. 2010;81:1088–95.
[24] Vogel AI. A text book of quantitative inorganic analysis. 3rd ed. London: Longmans; 1975.
[25] Jothieswari D, Anandakumar K, Santhi DV, Vijayakumar B, Priya D, Rathinaraj BS. A validated UV spectrophotometric method for the simultaneous estimation of amlodipine besylate, valsartan and hydrochlorothiazide in bulk and in combined tablet dosage rate. J Pharmaceut Biomed Sci. 2010;1–5.
[26] Kadadevarmath JS, Malimath GH, Melavanki RM, Patil NR. Static and dynamic model fluorescence quenching of laser dye by carbon tetrachloride in binary mixtures. Spectrochim Acta A. 2014;117:630–4.
[27] Nilchi A, Dehaghan TS, Garmarodi SR. Kinetics, isotherm and thermodynamics for uranium and thorium ions adsorption from aqueous solutions by crystalline tin oxide nanoparticles. Desalination. 2013;321:67–71.
[28] Wen J, Huang Z, Hu S, Li S, Li W, Wang X. Aggregation-induced emission active tetraphenylethene-based sensor for uranyl ion detection. J Hazard Mater. 2016;318:363.
[29] Shu X, Wang Y, Zhang S, Huang L, Wang S, Hua D. Determination of trace uranyl ion by thermoresponsive porphyrin-terminated polymeric sensor. Talanta. 2015;131:198.
[30] Yang CT, Han J, Gu M, Liu J, Li Y, Huang Z, et al. Fluorescent recognition of uranyl ions by a phosphorylated cyclic peptide. Chem Commun. 2015;51:11769.
[31] Elabd AA, Attia MS. A new thin film optical sensor for assessment of UO_2^{2+} based on the fluorescence quenching of trimetazidine doped in sol gel matrix. J Lumin. 2015;165:179–85.
[32] Elabd AA, Attia MS. Spectroflourimetric assessment of UO_2^{2+} by the quenching of the fluorescence intensity of Clopidogrel embedded in PMMA matrix. J Lumin. 2016;169:313–8.
[33] Elabd AA, Elhefnawy OA. An efficient and sensitive optical sensor based on furosemide as a new fluoroionophore for determination of uranyl ion. J Fluoresc. 2016;26:271–6.